JOURNAL OF MATERIALS SCIENCE 27 (1992) 5765–5768

Mechanical properties of hot-pressed SiC particulate-reinforced Al_2O_3 matrix

I. THOMPSON, V. D. KRSTIC
Department of Materials and Metallurgical Engineering, Queen's University, Kingston, Ontario, Canada K7L 3N6

The effect of SiC particulate dispersoids on the fracture toughness and strength of hot-pressed Al_2O_3-based composites was evaluated. Addition of 20 vol% SiC particulates was found to increase both the fracture toughness and strength of Al_2O_3. The relationships between mechanical properties and SiC additions are discussed.

1. Introduction

Ceramics have long been considered for use in structural components such as heat engines and other room- and high-temperature applications requiring good oxidation and corrosion resistance and high wear resistance. However, the limiting factor for wider use of ceramics has been their low fracture toughness and poor reliability in service. The production of ceramic–ceramic composites is at present the method which has the greatest potential for producing components with improved fracture toughness and susceptibility to catastrophic fracture. Since the first successful toughening of a glass matrix with brittle alumina particles [1] and metallic ductile particles [2], numerous investigations have shown that both fracture toughness and strength can be greatly increased when a ceramic matrix is reinforced with brittle particles. Typical examples are SiC–TiB_2 [3], SiC–TiC [4] and Si_3N_4–TiC [5] particulate composites. The major advantage of particulate composites over those of whiskers and fibres is the ease of fabrication and the ability to tailor the thermal and mechanical properties.

The present paper describes the effect of particulate SiC addition on the microstructure and mechanical properties of an Al_2O_3 matrix.

2. Experimental procedure

The Al_2O_3 powder used in this study (Grade A-16SG, Alcoa Co., Bauxite, Arkansas) had an average particle size of 0.3–0.5 μm and a surface area of 12 $m^2 g^{-1}$. The reinforcing material was high-purity β-SiC powder (A-10, H. C. Starck, Berlin) with a surface area of 13 $m^2 g^{-1}$ and an average particle size of 0.5 μm. Mixing of the powders was done by attrition milling in ethanol with an alumina milling media in order to prevent contamination. After milling, the slurry was dried in air for 8 h and then hot-pressed at 1850°C at a pressure of 35 MPa for 30 min.

The densities of the hot-pressed specimens were measured by the water displacement method. The theoretical densities of Al_2O_3 and SiC were taken as 3.99 and 3.21 $g cm^{-3}$, respectively.

Microstructure was examined by reflected light microscopy after sectioning and polishing. Grain structure was revealed by SEM fractography of polished surfaces etched in boiling 85% H_3PO_4 acid for 15 to 45 min.

The fracture toughness K_{IC} of samples machined from hot-pressed specimens was measured by the double countilever beam (DCB) method and the chevron notched four-point bend method [6]. The DCB samples were 48 mm long by 12 mm wide and 4 mm thick with a surface groove 1 mm wide and 1 mm deep. The specimens were precracked by wedge-loading and a penetrant dye was injected to facilitate accurate crack length measurements. Upon removing the excess dye, the specimens were dried overnight prior to testing.

The two remaining DCB specimens were subsequently machined into chevron notch beam (CVNB) specimens with dimensions 4 mm by 5 mm by 48 mm. The K_{IC} value was calculated using the Munz equation [6]. The CVND fracture toughness measurements were carried out at a crosshead speed of 0.05 mm min^{-1} with a jig having outer and inner spans of 40 mm and 20 mm, respectively.

Fracture strength measurements were performed using a four-point bending jig with outer and inner spans of 20 mm and 10 mm, respectively. A minimum of five samples were broken for each composition. The crosshead speed was 0.05 mm min^{-1}.

The grain size was measured using the three-circle procedure in accordance with ASTM standard E112-77.

Fractured and polished surfaces were examined using standard SEM.

3. Results and discussion

In order to minimize the effect of density on the mechanical properties of the composite, the sintered

0022–2461

density of the samples was kept within 2% difference. Table I displays the variation of density with volume fraction of SiC particles.

As expected, the lowest density was obtained with samples containing the highest amount of particulates. Fracture surface observations revealed that most of the SiC particles were uniformly distributed, with some particles concentrated along the alumina grain boundaries (Fig. 1). Their presence in the Al_2O_3 matrix appears to prevent grain-boundary migration and limit the grain growth. Fig. 2 shows the change of grain size with volume fraction of SiC particles. Inspection of Fig. 2 indicates that the grain size of the Al_2O_3 matrix drops from $\sim 15\ \mu m$ (for pure Al_2O_3) to less than $\sim 2\ \mu m$ for 20 vol % of SiC particles. Drastic reduction in grain size with the addition of SiC particles serves as a confirmation that the SiC particles had a grain growth inhibiting role. As expected, this reduction in grain size led to considerable improvements in strength (Fig. 3). With increasing volume fraction of SiC the fracture strength first increases, reaching a maximum value at approximately 15 vol % SiC, and then decreases. The increase in fracture strength with increasing volume fraction of SiC particulates appears to be in accordance with the strength–grain-size change for the unreinforced Al_2O_3 matrix (Fig. 4) [7].

Fracture toughness measurements, on the other hand, have shown practically no change of K_{IC} value up to 15 vol % SiC (Fig. 5). At 20 vol % SiC the fracture toughness increased to 4.7 MPa $m^{1/2}$, which is significantly larger than that of monolithic alumina of comparable grain size [8].

TABLE I Density of hot-pressed samples containing various amounts of SiC particles in Al_2O_3 matrix

Composition (% SiC)	Pressing temperature (°C)	T.D. (%)
5	1850	97.74
10	1850	97.36
15	1850	96.07
20	1850	96.03

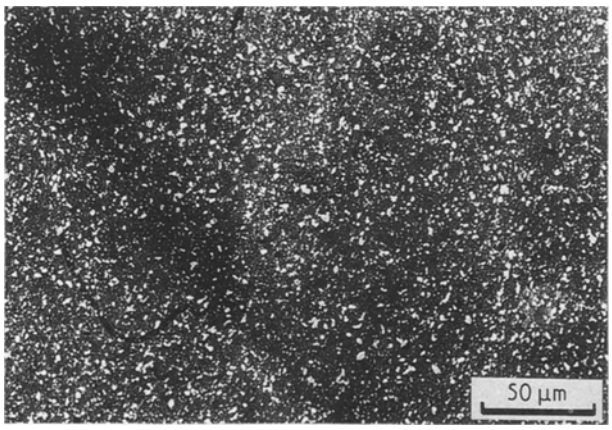

Figure 1 Optical micrograph of a hot-pressed sample containing 15 vol % SiC particles in Al_2O_3 matrix. White regions are SiC particles.

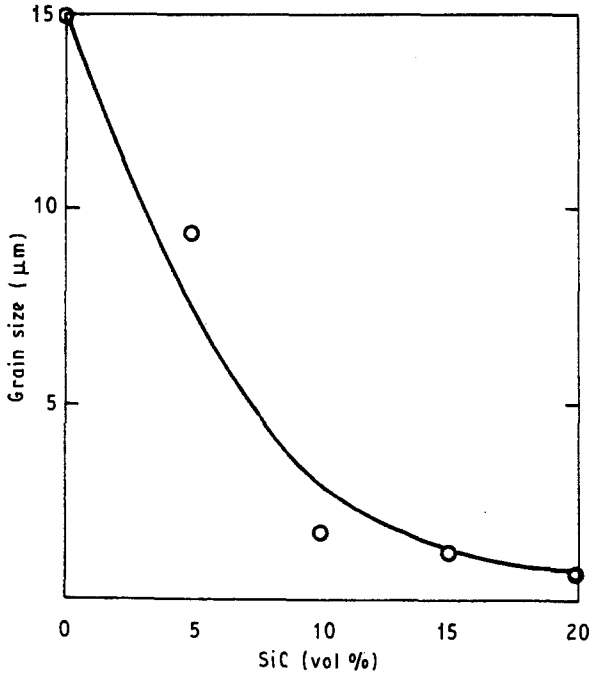

Figure 2 Change of grain size of Al_2O_3 matrix with addition of SiC particles.

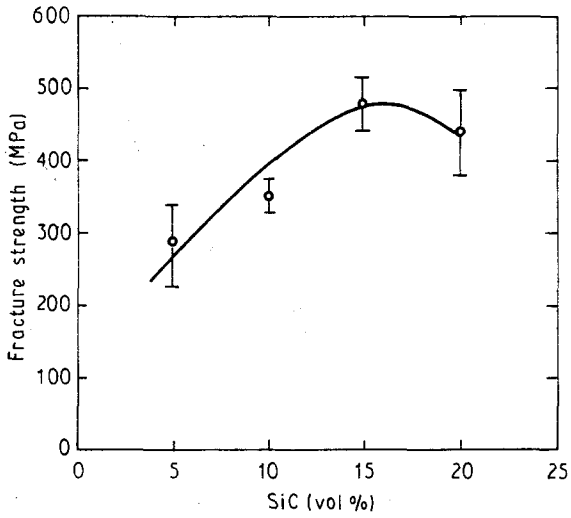

Figure 3 Fracture strength versus volume fraction of SiC in Al_2O_3 matrix.

The increase in fracture toughness of the composite at 20 vol % SiC is believed to be associated with the presence of residual thermoelastic stresses generated as a result of thermal and elastic mismatch. The difference in thermal expansion coefficients between Al_2O_3 ($\alpha = 8.9 \times 10^{-6}\ °C^{-1}$) and SiC ($\alpha = 4.8 \times 10^{-6}\ °C^{-1}$) is expected to generate large compressive stresses in the SiC particles and a corresponding tensile (tangential to the particle) stresses in the Al_2O_3 matrix. For particles of spherical shape, uniformly distributed in an infinite matrix, these stresses can be calculated from the following expressions:

$$\sigma_r = -2\sigma_\theta = P\left(\frac{R}{r}\right)^3. \quad (1)$$

where σ_r is the radial and σ_θ the tangential component of the stress outside a spherical particle, R is the

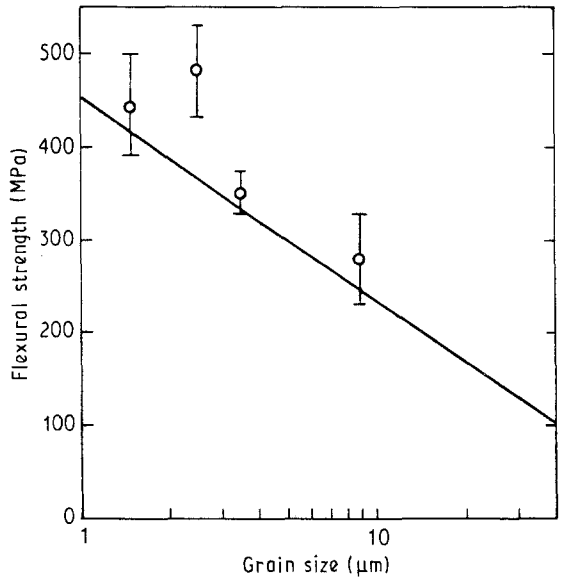

Figure 4 Change of fracture strength with grain size for (——) hot-pressed monolithic Al_2O_3 (from [7]) and (○) hot-pressed alumina reinforced with SiC particles (present work).

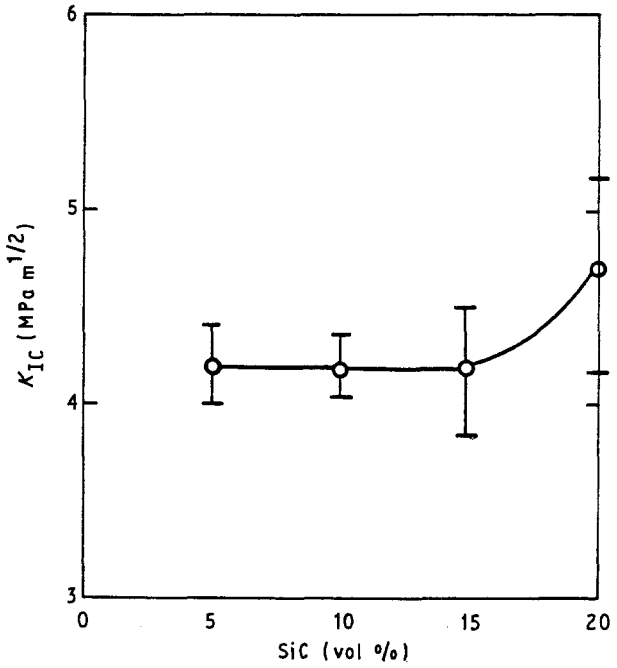

Figure 5 CVNB fracture toughness as a function of volume fraction of SiC particles in Al_2O_3 matrix.

particle radius, r is the distance from the centre of the particle and

$$P = \frac{(\alpha_m - \alpha_p)\Delta T}{(1 + \nu_m)/2E_m + (1 - 2\nu_p)/E_p} \quad (2)$$

In Equation 2, α_m, ν_m, E_m and α_p, ν_p, E_p are the coefficients of thermal expansion, Poisson's ratios and Young's moduli for the matrix and particle, respectively. Assuming $\nu_m = \nu_p = 0.25$, and using $E_p = 440$ GPa and $E_m = 350$ GPa, one finds that for $\Delta T = 900°C$, substantial matrix stresses can be developed ($\sigma_\theta = +631$ MPa compressive and $\sigma_r = -1263$ MPa tensile). Evidently these stresses are significantly larger than the fracture stress of a polycrystalline alumina, suggesting that some stress relaxation within the matrix must have occurred. If no stress-field interaction between the neighbouring particles exists, the critical particle size for spontaneous cracking in the presence of thermoelastic stresses may be obtained from the expression [9]

$$D_c = \frac{\pi E_m \gamma_f}{P^2}\left(\frac{R}{a}\right)\left[1 - \left(1 - \frac{R^2}{a^2}\right)^{1/2}\right]^{-2} \quad (3)$$

where γ_f is the effective fracture surface energy and a is the half crack length (comprising the particle radius and an annular flow size). Substituting values for a single-crystal fracture energy $\gamma_f = 6\,J\,m^{-2}$, $E_m = 350$ GPa, $P = 1263$ MPa and $R/a = 0.9$ in Equation 3, gives $D_c \simeq 12$ μm. This calculated critical particle size for spontaneous cracking is two to six times larger than the measured particle size ($D \simeq 2$–5 μm). However, microcracking may occur at larger volume fractions of particles (> 5–10%) where the stress-field interaction effects start to control the microcracking condition. It is of interest to note that when the SiC addition is less than ~ 15 vol % the fracture strength increases gradually with increasing volume fraction of SiC, reaching a maximum at ~ 15 vol % SiC. It is possible that there is a critical volume fraction of SiC addition which causes crack link-up or coalescence [10, 11]. An assessment of the effect of the crack-tip stress fields interaction of neighbouring cracks, and the particle volume fraction at which crack link-up occurs, may be obtained from the equation which relates the stress intensity factor for an infinite row of cracks perpendicular to the applied stress (K_I^m) and the stress intensity factor for a single crack (K_I^s) [12]:

$$K_I^m = K_I^s\left(\frac{\pi a}{2b}\right)^{-1/2}\left(\tan\frac{\pi a}{2b}\right)^{1/2} \quad (4)$$

where b is the distance between the centres of the cracks and a is the half crack length. It has been found that the stress intensity factor of an annular crack of length s emanating from the particle–matrix interface is a function of particle size [9]:

$$K_I^s = 2P\left(\frac{R}{\pi}\right)^{1/2}\left(1 + \frac{s}{R}\right)^{1/2} \times\left[1 - \left(1 - \frac{1}{[1 + (s/R)]^2}\right)^{1/2}\right] \quad (5)$$

Substitution of Equation 5 in Equation 4, and replacing b with $R + s + (d/2)$ and a with $R + s$, gives

$$K_I^M = 2P\left(\frac{R}{\pi}\right)^{1/2}\left(1 + \frac{s}{R}\right)^{1/2} + \left[1 - \left(1 - \frac{1}{[1 + (s/R)]^2}\right)^{1/2}\right] \times\left(\frac{\pi[1 + (s/R)]}{2[1 + (s/R) + 1(1 - V)/3V]}\right)^{-1/2} \times\left(\tan\frac{\pi[1 + (s/R)]}{2[1 + (s/R) + 2(1 - V)/3V]}\right)^{1/2} \quad (6)$$

where V is the volume fraction of particles and d is the

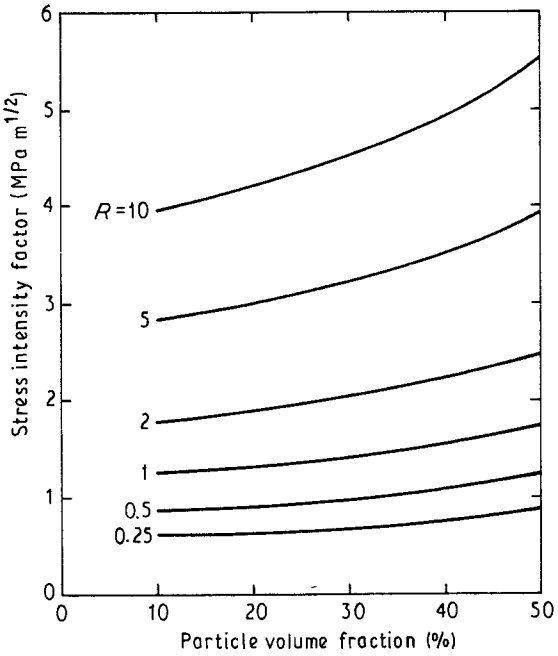

Figure 6 Predicted variation of stress intensity factor (from Equation 6) with volume fraction of SiC particles in Al_2O_3 matrix for $s/R = 0.01$.

intercrack separation. Fig. 6 illustrates the predicted change of stress intensity factory (from Equation 6) with volume fraction of SiC in an Al_2O_3 matrix for a given particle size. Fig. 6 and Equation 6 show that for a given particle size, s/R, and P value, crack extension will occur when K_I^M attains a critical value (K_{IC}^M) for a monolithic, polycrystalline Al_2O_3 matrix. The fracture toughness of a polycrystalline Al_2O_3 was found to vary from $\sim 2\,MPa\,m^{1/2}$ for a single-crystalline material to $\sim 5.3\,MPa\,m^{1/2}$ for a polycrystalline coarse-grained Al_2O_3 [13]. If single-crystal fracture energy is used, the critical volume fraction required to initiate crack extension will be $\sim 30\%$ for particles of 2 μm size. If, however, a polycrystalline fracture energy is used (i.e. $K_{IC}^M = 5.3\,MPa\,m^{1/2}$), the size of SiC particles required to induce cracking will increase to > 6 μm. For particles of ~ 10 μm size, for example, the critical volume fraction for microcracking will be $\sim 40\%$.

It should be pointed out that the above analysis is limited to cases where there is no change of s/R with particle size or volume fraction. For cases where there is an increase in s/R with particle size and/or volume fraction, the critical volume fraction for microcracking will be smaller and the critical grain size will be larger than predicted.

4. Conclusions

The addition of submicrometre size SiC particulates to an Al_2O_3 matrix increased both the fracture toughness and strength. The maximum in strength was found at 15 vol % SiC addition. The increase of strength with SiC addition was found to be the result of a decrease in grain size of the Al_2O_3 matrix. At small particle volume fractions (below approximately 15%), the residual thermoelastic stress is insufficient to initiate cracks on cooling from the hot-pressing temperature. At large volume fractions ($> 15\%$) of SiC particulates, the stress-field interaction of neighbouring particles plays the dominant role in controlling the microcracking condition. This conclusion is supported by the observed drop in strength above ~ 15 vol % SiC particulates and an increase in toughness. The increase in fracture toughness above 15 vol % SiC is ascribed to matrix microcracking, with some possible contribution from crack deflection.

References

1. F. F. LANGE, *J. Amer. Ceram. Soc.* **54** (1971) 614.
2. V. D. KRSTIC, P. S. NICHOLSON and R. G. HOAGLAND, *ibid.* **64** (1981) 499.
3. C. H. McMURTRY, W. D. G. BOECKER, S. G. SESHADRI, J. S. ZANGHIE and J. E. GARNIER, *Amer. Ceram. Soc. Bull.* **66** (1987) 325.
4. G. C. WEI and P. F. BECKER, *J. Amer. Ceram. Soc.* **67** (1984) 571.
5. T. MAH, M. G. MENDIRATTA and H. LIPSITT, *Amer. Ceram. Soc. Bull.* **60** (1981) 1229.
6. D. MUNZ, *Int. J. Frac.* **16** (1980) R137.
7. E. M. PASSMORE, R. M. SPRIGGS and T. VASILOS, *J. Amer. Ceram. Soc.* **48** (1965) 1.
8. R. W. RICE, S. W. FREIMAN and P. F. BECHER, *ibid.* **64** (1981) 345.
9. V. D. KRSTIC and M. D. VLAJIC, *Acta. Metall.* **31** (1983) 139.
10. B. CORNWALL and V. D. KRSTIC, *J. Mater. Sci.* **27** (1992) 1217.
11. J. WANG and R. STEVENS, *ibid.* **24** (1989) 3421.
12. P. C. PARIS and G. C. SIH, "Fracture Toughness Testing and its Applications", ASTM STP 381 (American Society for Testing and Materials, Philadelphia, 1964), p. 30.
13. R. W. RICE and R. C. POHANKA, *J. Amer. Ceram. Soc.* **62** (1979) 559.

Received 23 July 1991
and accepted 4 February 1992